Cell-free Layer Measurements in Bifurcating Microchannels: a global approach

B. Taboada*, D. Bento*, D. Pinho*, A.I. Pereira‡, R. Lima*

*Instituto Politécnico de Bragança, Portugal & CEFT, Faculty of Engineering at University of Porto, Portugal.
E-mail:{ brunataboada, davidbento, diana, ruimec}@ ipb. pt

‡ Instituto Politécnico de Bragança, Portugal & Algoritmi, Universidade do Minho, Portugal.
E-mail:apereira@ ipb. pt

Abstract

In the present work, *in vitro* blood flowing through bifurcating microchannels was studied, with the aim of characterizing the cell-free layer (CFL). The original images were obtained by means of a high-speed video microscopy system and then processed in MatLab using the Image Processing Toolbox. The numerical data was obtained automatically and analyzed by optimization techniques using the genetic algorithm approach. The results suggest that the CFL were formed in a similar way at the upper and lower regions in all bifurcations, and the measurements can be approximated through a sum of trigonometric functions.

Keywords: Cell-free Layer. Image Processing. Nonlinear Optimization. Global Optimization.

1   Introduction

Blood flow in microcirculation shows several hemodynamic phenomena that happen at both, *in vivo* and *in vitro* blood flowing. Hence, over the years *in vitro* blood studies in microchannels have been extensively performed in order to obtain an understanding of blood rheology and its flow dynamics [Goldsmith et al., 1989, Pires et al., 1992, Lima et al., 2012]. A well known hemodynamic phenomenon observed in both studies, *in vivo* and *in vitro*, states that for narrow microtubes ($< 300 \ \mu m$) both hematocrit (Hct) and apparent blood viscosity decreases as the tube diameter is reduced [Goldsmith et al., 1989, Pires et al., 1992, Lima et al., 2012]. The physical reasons for these phenomena and for the formation of the cell-free layer (CFL), is known as Fahraeus-Lindqvist effect that is the tendency of red blood cells (RBCs) to migrate toward the centre of the microtube resulting in a marginal CFL at regions adjacent to the wall [Caro et al., 1978]. Recently several studies showed strong evidence that the formation of the CFL is affected by the geometry of the microchannel [Pinho, 2011, Lima et al., 2008a, Lima et al., 2008b, Leble et al., 2011] and the physiological conditions of the working fluid, such as the hematocrit [Garcia et al., 2012, Fujiwara et al., 2009].

Although there have been several studies on the measurement of CFL thickness [Namgung et al., 2010, Kim et al., 2006] according to our knowledge there have been very few studies on the determination of CFL measurements [Bento et al., 2012, Bento et al., 2013]. For these studies image analysis is extremely important to obtain crucial information [Pinho et al., 2012].

The main purpose of the present work is to measure the CFL in a microchannels with bifurcations by means of an automatic method developed in MatLab [Bento et al., 2012, Bento et al., 2013], and characterize the CFL along this microchannel using global optimization techniques.

The paper is organized as follows. The Section 2 presents the materials used in this work and the methods that were applied in this study. The Section 3 presents a brief description of the genetic algorithm. The Section 4 presents the numerical results and some discussion. The last section presents some conclusions and future work.

2   Materials and Methods

2.1   Experimental set-up

The high-speed video microscopy system used in this study consists of an inverted microscope (IX71; Olympus) combined with a high-speed camera (i-SPEED LT). The microchannel was placed on the stage

of the inverted microscope and by using a syringe pump (PHD ULTRA) a pressure-driven flow was kept constant (cf. Figure 1).
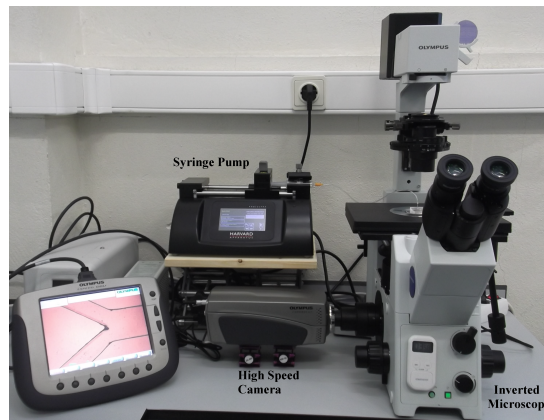

Figure 1: High-speed video microscopy system used in this staudy.

The series of microscope images were captured with a resolution of 600×800 pixels. All the images were recorded at the center plane of the microchannels at a rate of 200 frames/second and were transferred to the computer and then evaluated using image analysis techniques.

2.2   Working fluids and microchannel geometry

The blood samples used were collected from a healthy adult sheep, and ethylenediaminetetraacetic acid (EDTA) was added to prevent coagulation. The red blood cells (RBCs) were separated from the blood by centrifugation and washed twice with physiological saline (PS). The washed RBCs were suspended in Dextran 40 (Dx 40) to make up the required RBCs concentration by volume - hematocrit. In this study the Hct of 10% was used. All blood samples were stored hermetically at $4^\circ C$ until the experiment was performed.

The microchannels fabricated for the proposed study have been produced in PDMS by a soft-lithography technique. The geometry used is a network of microchannels, containing several bifurcations and confluences. Figure 2 illustrates the configuration of the network and the regions where the CFL was measured.
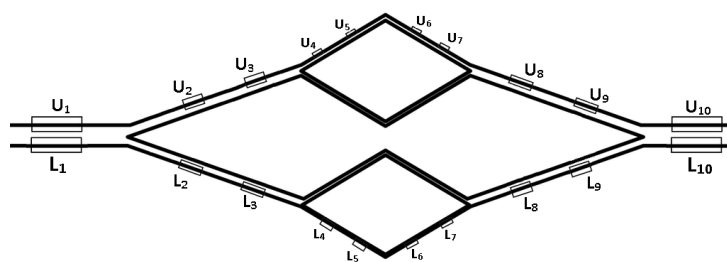

Figure 2: The geometry of the network and the regions where the CFL was measured.

2.3   Image Analysis

All image sequences, like Figure 3, were processed using Image Processing toolbox, available in MatLab [Matlab, 2002], and an automatic method was developed and tested [Bento et al., 2013]. The method consists in the combination of binarization of all images sequence and evaluation of all pixels using the maximum intensity.

Firstly a median filter with a 3×3 pixel mask was applied to each frame to reduce the noise, and then, the intensity of each pixel in the frame sequence was evaluated to obtain an image with the maximum intensity, as is possible to observe in Figure 4.
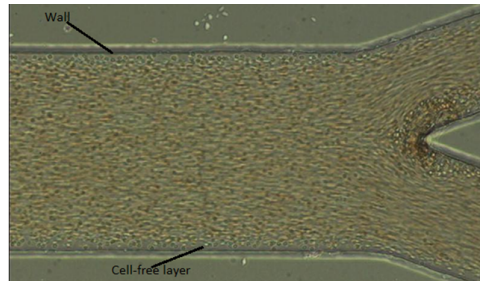
Figure 3: The original image of blood sample flowing in a bifurcating microchannel.
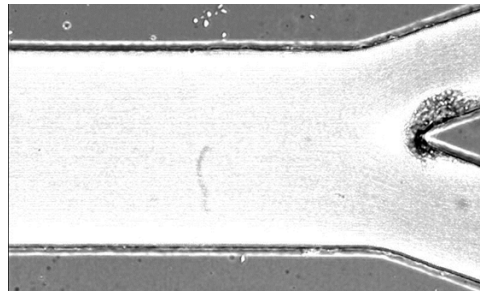

Figure 4: The image after the evaluation with the maximum intensity.

With this last step it is possible to identify the region of the concentration of blood cells (RBC core) and the region where blood cells do not exist, the cell-free layer. As the final step the image (Figure 4) was converted into a binary image. Finally, the region of interest is selected and the upper and lower CFLs are automatically measured. Figure 5 represents the image after binarization.
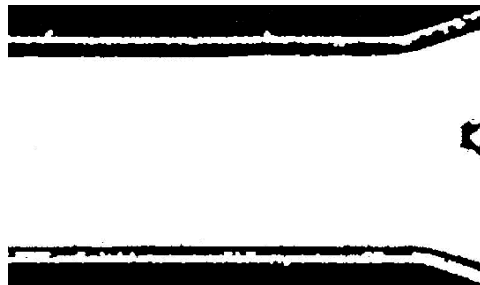

Figure 5: Binary image which shows clearly the boundary of CFL and RBC core.

3   Global optimization method: Genetic Algorithm

In the present work the genetic algorithm (GA) was used. The GA is an optimization technique based on the principles of evolution, this method allows to find a global minimum in a large search space. Given an individual, that is defined by the genes, this method creates new generations through analysis of the individuals genes from previous generations and selecting the best ones by applying the fitness function.

The GA uses crossover process, where the genes of the best individuals are crossed with genes from other individuals which also have good performance. The GA also applies the concept of mutation, improving the optimization process by introduction values that were not present in the previous generations.

This technique does not guarantee that the global minimum is found, however it is accepted that the final solution is close to the global minimum provided that successive generations cannot produce better individuals [Catlin et al., 2011].

4   Results and Discussion

The captured videos were analyzed and the numerical data was taken in the regions already defined in Figure 2. The flow rate used was 500 nl/min and one fluid was studied with 10% of Hct.

To fit the numerical data the nonlinear least squares theory was used. In each region U_i, for $i = 1, ..., 10$, and L_i, for $i = 1, ..., 10$, we applied the nonlinear optimization problem defined as follows

$$\min \quad f(y) \equiv \sum_{k=1}^{N_R} \left(M_k - g_h(y, x_k) \right)^2 \tag{4.1}$$

$$s.t \quad g_h(y, x_k) \geq 0 \ \forall k = 1, ..., N_R$$

where (x_k, M_k), for $k = 1, ..., N_R$ are the CFL measurements of the region R (defined as U_i and L_i, for $i = 1, ..., 10$). The functions g_h, for $h = 1, ..., 3$, are defined as follows

$$\begin{aligned} g_1(y, x) &= y_1 x^2 + y_2 x + y_3, \\ g_2(y, x) &= y_1 x + y_2, \\ g_3(y, x) &= sin(y_1 x) + cos(y_2 x) + y_3. \end{aligned} \tag{4.2}$$

The following table presents the obtained numerical results using the genetic algorithm to solve the optimization problem (4.1). Since the genetic algorithm is a stochastic method, each problem was solved 30 times. Table 1 presents the regions where the problem (4.1) was applied, the average of the optimum value and the minimum value obtained in the all 30 runs.

Table 1: Numerical results obtained using genetic algorithm.

	Upper cell-free layer				Lower cell-free layer		
Region	Function	Average	Minimun	**Region**	Function	Average	Minimun
U$_1$	g_1	2.71×10^7	8.14×10^3	**L$_1$**	g_1	1.13×10^7	1.05×10^5
	g_2	2.17×10^3	1.91×10^3		g_2	1.41×10^3	1.34×10^3
	g$_3$	**1.90×10^3**	**1.50×10^3**		**g$_3$**	**1.19×10^3**	**1.00×10^3**
U$_2$	g_1	4.29×10^7	2.86×10^3	**L$_2$**	g_1	4.63×10^6	2.36×10^3
	g_2	1.27×10^3	4.02×10^2		g_2	2.32×10^3	2.07×10^3
	g$_3$	**7.68×10^2**	**5.38×10^2**		**g$_3$**	**2.31×10^3**	**1.85×10^3**
U$_3$	g_1	1.32×10^8	5.99×10^3	**L$_3$**	g_1	9.30×10^6	3.44×10^3
	g_2	4.76×10^3	1.67×10^3		g_2	3.34×10^3	3.06×10^3
	g$_3$	**1.92×10^3**	**1.60×10^3**		**g$_3$**	**2.81×10^3**	**2.36×10^3**
U$_4$	g_1	2.88×10^6	1.14×10^4	**L$_4$**	g_1	4.61×10^7	9.63×10^4
	g_2	1.27×10^3	1.21×10^3		g_2	5.97×10^3	5.18×10^3
	g$_3$	**9.94×10^2**	**7.75×10^2**		**g$_3$**	**4.61×10^3**	**4.07×10^3**
U$_5$	g_1	1.30×10^7	1.68×10^3	**L$_5$**	g_1	1.28×10^7	2.26×10^3
	g_2	1.77×10^3	1.62×10^3		**g$_2$**	**2.38×10^3**	**2.04×10^3**
	g$_3$	**1.43×10^3**	**1.20×10^3**		g_3	3.74×10^3	3.35×10^3
U$_6$	g_1	2.61×10^6	2.66×10^3	**L$_6$**	g_1	8.35×10^6	5.49×10^3
	g_2	6.07×10^2	5.02×10^2		g_2	9.12×10^3	5.46×10^3
	g$_3$	**3.70×10^2**	**3.31×10^2**		**g$_3$**	**1.31×10^3**	**9.90×10^2**
U$_7$	g_1	1.18×10^7	3.73×10^4	**L$_7$**	g_1	6.90×10^5	3.53×10^3
	g_2	8.65×10^2	6.53×10^2		g_2	4.91×10^3	2.71×10^3
	g$_3$	**6.45×10^2**	**5.28×10^2**		**g$_3$**	**3.30×10^3**	**2.55×10^3**
U$_8$	g_1	1.53×10^7	1.20×10^4	**L$_8$**	g_1	3.32×10^7	8.49×10^4
	g_2	2.72×10^3	1.62×10^3		**g$_2$**	**2.96×10^3**	**1.31×10^3**
	g$_3$	**1.82×10^3**	**1.34×10^3**		g_3	3.90×10^3	2.76×10^3
U$_9$	g_1	1.58×10^8	2.73×10^3	**L$_9$**	g_1	2.10×10^8	7.36×10^4
	g_2	1.24×10^3	9.09×10^2		**g$_2$**	**1.52×10^3**	**9.08×10^2**
	g$_3$	**1.10×10^3**	**8.30×10^2**		g_3	1.59×10^3	1.09×10^3
U$_{10}$	g_1	1.21×10^7	1.64×10^4	**L$_{10}$**	g_1	2.29×10^8	3.08×10^3
	g_2	2.03×10^3	1.74×10^3		g_2	3.04×10^3	2.41×10^3
	g$_3$	**1.77×10^3**	**1.38×10^3**		**g$_3$**	**2.19×10^3**	**1.81×10^3**

The numerical results suggested that the function g_3 fits better the CFL boundary, since the minimum value was obtained for this function. Other important fact is that the boundary has the same behavior in all bifurcations. The only exception was verified in the regions L_5, L_8 and L_9, in these regions the best fit was obtained with the function g_2.

5   Conclusions and Future Work

In this study, we present a method to obtained automatically the CFL measurements. The CFL boundary was fitted using three different functions. The genetic algorithm was used to solve the constrained optimization problem. The best fit was obtained using the function g_3, i.e. a sum of trigonometric functions. As future work, we will test more fluids with different properties and different functions to fit the CFL measurements.

Acknowledgments

References

[Bento et al., 2013] Bento, D., Pinho, D., Pinto, E., Tomoko, Y., Correia, T., Lima, J., Pereira, A.I., Lima, R. (2013). Cell-free layer measurements in a bifurcation microchannel: comparison between a manual and automatic methods. 5th Portuguese Congress on Biomechanics: 359-362.

[Bento et al., 2012] Bento, D., Pinho, D., Pereira, A., Lima, R. (2012) Cell-Free Layer (CFL) Analysis in a Glass Capillary: Comparison Between a Manual and Automatic Method. AIP Conference Proceedings 1479: 786-789.

[Caro et al., 1978] Caro, C., Pedley, T., Schroter, R., Seed, W. (1978). The mechanics of the circulation. *Oxford University Press*.

[Catlin et al., 2011] Catlin, G., Advani, S., Prasad, A. (2011). Optimization of polymer electrolyte membrane fuel cell channels using a genetic algorithm. *Journal of Power Sources*, 196:9407–9418.

[Fujiwara et al., 2009] Fujiwara, H., Ishikawa, T., Lima, R., Matsuki, N., Imai, Y., Kaji, H., Nishizawa, M., Yamaguchi, T. (2009). Red blood cells motions in high-hematocrit blood flowing through a stenosed microchannel. *Journal of Biomechanics*, 42:838–843.

[Garcia et al., 2012] Garcia, V., Dias, R., Lima R. (2012). In Vitro Blood Flow Behaviour in Microchannels with Simple and Complex Geometries. *Journal of Biomechanics Applied Biological Engineering - Principles and Practice, Ganesh R. Naik (ed.), InTechcs*, 17:394–416.

[Goldsmith et al., 1989] Goldsmith, H., Cokelet, G., Gaehtgens, P. (1989). Robin Fahraeus: evolution of his concepts in cardiovascular physiology. *American Journal of Physiology*, 257:H1005–H10015.

[Kim et al., 2006] Kim, S., Kong, R. L., Popel, A. S., Intaglietta, M., Jonhson J. C.(2006). A computer-based method for determination of the cell-free layer width in microcirculation. *Microcirculation*, 13:199-207.

[Leble et al., 2011] Leble, V., Lima, R., Dias, R. P., Fernandes, C. S., Ishikawa, T., Imai, Y., Yamaguchi, T. (2011). Asymmetry of red blood cell motions in a microchannel with a diverging and converging bifurcation. *Biomicrofluidics*, 5:044120.

[Lima et al., 2008a] Lima, R., Wada, S., Tanak, S., Takeda, M. (2008). In vitro blood flow in a rectangular PDMS microchannel: experimental observations using a confocal micro-PIV system. *Biomedical Microdevices*, 10(2):153–167.

[Lima et al., 2008b] Lima, R., Ishikawa, T., Imai, Y. (2008). Radial dispersion of red blood cells in blood flowing through glass capillaries: role of hematocrit and geometry. *Journal of Biomechanics*, 41:2188-2197.

[Lima et al., 2012] Lima, R., Ishikawa, T., Imai, Y., Yamaguchi, T. (2012) Single and two-phase flows on Chemical and Biomedical Engineering. Bentham Science, Dias et al., 513-547.

[Matlab, 2002] Eddins, S. L., Gonzalez, R. C., Woods, R. E. (2002). Digital Image Processing Using Matlab. *MathWorks*.

[Namgung et al., 2010] Namgung, B., Ong, P. K., Wong, Y. H., Lim, D., Chun, K. C., Kim, S. (2010). A comparative study of histogram-based thresholding methods for the determination of cell-free layer width in small blood vessels. *Physiological Measurement*, 31:N61–N70.

[Pinho, 2011] Pinho, D. (2011). Determination and characterization of red blood cells trajectories: a semi-automatic method. *Master in Biomedical Technology, Polytechnic Institute of Bragança, Portugal, 2011 (in portuguese)*.

[Pinho et al., 2012] Pinho, D., Lima, R., Pereira, A. I., Gayubo, F. (2012). Automatic tracking of labeled red blood cells in microchannels. *International Journal for Numerical Methods in Biomedical Engineering*, DOI: 10.1002/cnm.

[Pires et al., 1992] Pires, A. A., Neuhaus, D., Gaehtgens P. (1992). Blood viscosity in tube flow: dependence on diameter and hematocrit. *American Journal of Physiology*, 263:H1770–H1778.